WELDING RESEARCH

SUPPLEMENT TO THE WELDING JOURNAL, JUNE, 1982

Sponsored by the American Welding Society and the Welding Research Council

The Effect of Electrical Resistance on Nugget Formation During Spot Welding

Applying a higher resistance coating to HSLA steel increases the welding current range to an acceptable level and permits a reduction in electrode force

BY J. G. KAISER, G. J. DUNN AND T. W. EAGAR

ABSTRACT. Many high strength-low alloy (HSLA) steels are more difficult to resistance spot weld than low carbon steel, due primarily to the narrower welding lobe width. In order to understand the shape of the welding lobe, a comparison was made between HSLA and low carbon steel sheets. Three separate surface conditions on each sheet were studied. These conditions produced surface resistances which varied by approximately an order of magnitude between the lowest and the highest values.

Static resistances were measured with forces of 150 to 1700 lb (0.67 to 7.56 kN) using test currents of 1 to 1000 amperes. It was found that the static resistance values changed markedly with both force and test current. The contact resistance range for all samples spanned five orders of magnitude. It is shown that the static resistance measurements are controlled by the flattening and melting of surface asperites.

Welding lobes were measured at three or more force levels for each steel and surface condition. The shape and shift of these lobes with welding current can be explained in terms of the heat generated at the faying surface and in the bulk. A model of the local heat generation is proposed that divides a typical lobe into approximately four regimes, depending upon the dominance of either bulk or surface heating. The model provides a qualitative description of the lobe shape, and predictions from the model have been used to increase the acceptable welding current range of HSLA steels.

The initiation of surface melting has been studied in the scanning electron microscope. Three types of surface heating are observed depending upon the current/time parameters which are used. Each type is explained in terms of local surface conditions, local heat generation rate and heat transport in the metal.

Introduction

There has been great interest for many years in the use of high strength sheet steels, particularly as a means of reducing the weight of automobiles. For a number of reasons, the use of these materials has grown at a slower rate than originally anticipated. One of the limiting factors has been the more restricted range of acceptable welding parameters.

The nature of mass production spot welding requires the ability to make thousands of welds without machine readjustment. This reproducibility is hindered by inconsistencies in metal composition, by variation in surface finish and by electrode tip mushrooming. To allow for these changes during a welding run, it is desirable to use material with the greatest welding current range.

Unfortunately, many high strength steels have very narrow welding current ranges. In some cases, this restricted weldability is due to interfacial failure of the weld nugget (Ref. 1), resulting in an apparently smaller fusion zone. Other investigators have shown that high strength steels may be more susceptible to expulsion due to their higher electrical resistivity (Ref. 2), although the higher resistivity permits welds to be produced at lower currents (Ref. 3), which is considered an advantage. Still other investigators have found significant effects of prior surface preparation on spot weldability (Ref. 4, 5).

The problem addressed in this study is fundamental; it is desired to identify the material properties which control lobe width and to determine the manner in which these properties interact with the welding parameters. The independent process parameters chosen were pressure, time and current; the material properties studied were bulk resistance and surface resistance.

The total welding resistance may be thought of as a series resistance of five loads. These are the two electrode-sheet interface resistances, R_1 and R_5; the two bulk material resistances, R_2 and R_4; and the faying interface resistance, R_3. The interface resistances are determined by the thermal, electrical and mechanical behavior of the surface of the material. The faying resistance, R_3, drops to zero as the nugget is formed. An initial assumption of this work is that it is the dynamic interaction of these five resistances which determines the lobe width.

Based on a paper presented at the 62nd AWS Annual Meeting held in Cleveland, Ohio, during April 5-10, 1981.

J. G. KAISER, G. J. DUNN and T. W. EAGAR are associated with the Department of Materials Science and Engineering, Massachusetts Institute of Technology, Cambridge, Massachusetts.

Experimental

Starting Materials

The compositions of the two steels used in this study are given in Table 1. Both sheets were 1.2 mm (0.049 in.) thick. For each composition, surface conditions of high, medium and low resistance were studied. For both low carbon and HSLA, a low surface resistance was achieved by degreasing in trichlorethylene followed by pickling in separate baths of sulfuric acid and hydrochloric acid, completed by an alcohol rinse and drying. Several other pickling solutions and rinsing agents, as well as mechanical polishing and sandblasting techniques, were evaluated, but the procedure described above gave the lowest and the most consistent surface resistance. Due to the unprotected nature of the steel surface, the contact resistance increases after exposure to the atmosphere; hence, it was necessary to perform the welding tests immediately after pickling.

An intermediate value of surface resistance was achieved for both compositions by welding in the as-received condition. In this state, mill oil and light oxide were apparent on the steel surface.

A high resistance surface was prepared by either maintaining the sheet at 121°C (250°F) for 96 hours (h) under humid conditions or by application of a phosphate coating.

Welding Procedure

All welds were produced on a 75 kVA pneumatically operated resistance welding machine equipped with synchronous controls. RMS current values were determined, without the use of blanking, on a commercially available current meter (Duffers model no. 273). Dynamic force readings were produced by mounting a full bridge strain gage on the head cross bar of the welding machine. This was calibrated using a 1 in. (25.4 mm) diameter proving ring mounted between the electrode tips. Strain readings of the ring had been calibrated between similar tips using an Instron testing machine in the compressive mode. An electrode tip diameter of 6.3 mm (¼ in.) was used throughout the study, as was a 30 cycle hold time.

Table 1—Chemical Compositions of the Low Carbon and HSLA Steels Used in This Study, Wt-%

	Low carbon steel	HSLA steel
C	0.06	0.05
Mn	0.32	0.42
P	0.009	0.010
S	0.019	0.019
Si	0.004	0.28
Al	0.056	0.060
N	0.006	–
Nb	–	0.044

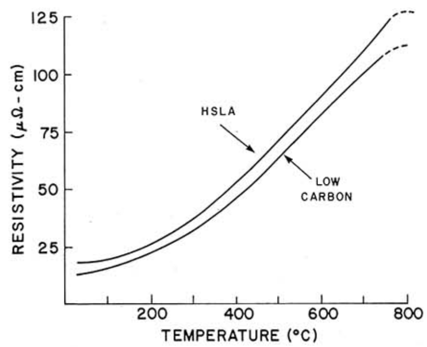

Fig. 1 — Bulk resistivity vs. temperature of both steels used in this study as measured with a four point probe

Welding lobes were determined for all six combinations of composition and surface treatment, using 100 by 25 mm (4 by 1 in.) coupons. The maximum current was determined when the shunting effect of a second weld produced the expulsion/no expulsion condition. The minimum welding current was measured by a peel test to determine the minimum acceptable nugget diameter.

Since electrode force directly affects the magnitude and the response of interface resistance, a high, medium (optimum) and low force lobe was constructed for each resistance combination. Thus a 2 × 3 × 3 matrix (composition, surface preparation and electrode force) of conditions was studied.

Static Resistance Measurements

In order to determine the effect of resistance on weld formation, it was necessary to isolate the influence of pressure and current on surface resistance. A DC circuit was constructed which enabled from one to 1000 amperes (A) to be pulsed between the electrode tips in the machine. The secondary circuit of the welding machine was excluded from the DC circuit by seating a specially designed tip in a teflon spacer thus insulating it from the machine. Voltage across the weld pieces was monitored from leads on the sides of the electrodes. Power was supplied by a 2000 A-h battery in series with a graphite plate rheostat.

The average resistance and standard deviation was calculated from approximately 20 measurements for each materi-

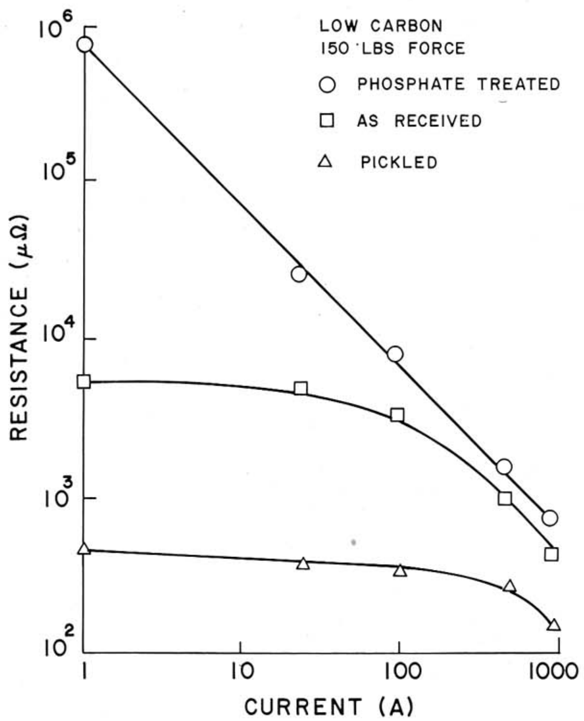

Fig. 2 — Static contact resistance as a function of test current for the carbon steel with three different surface conditions

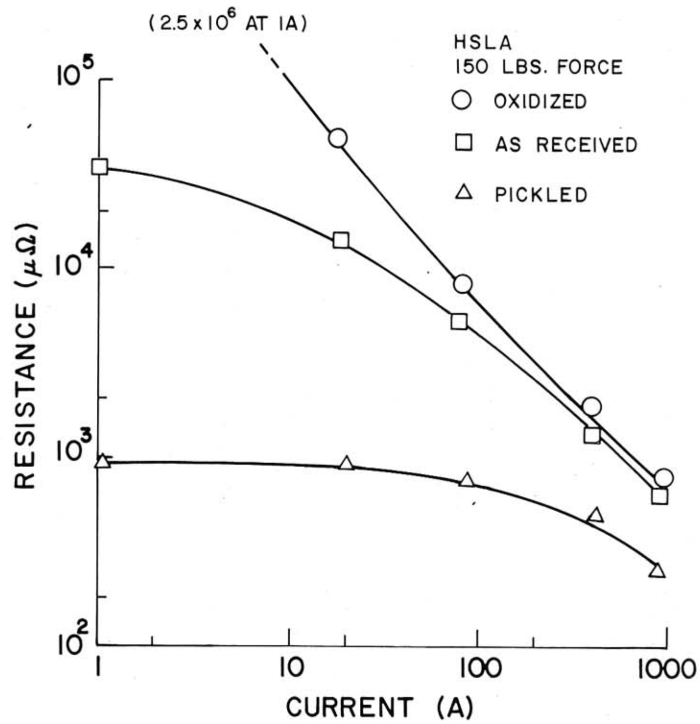

Fig. 3 — Static contact resistance as a function of test current for the HSLA steel with three different surface conditions

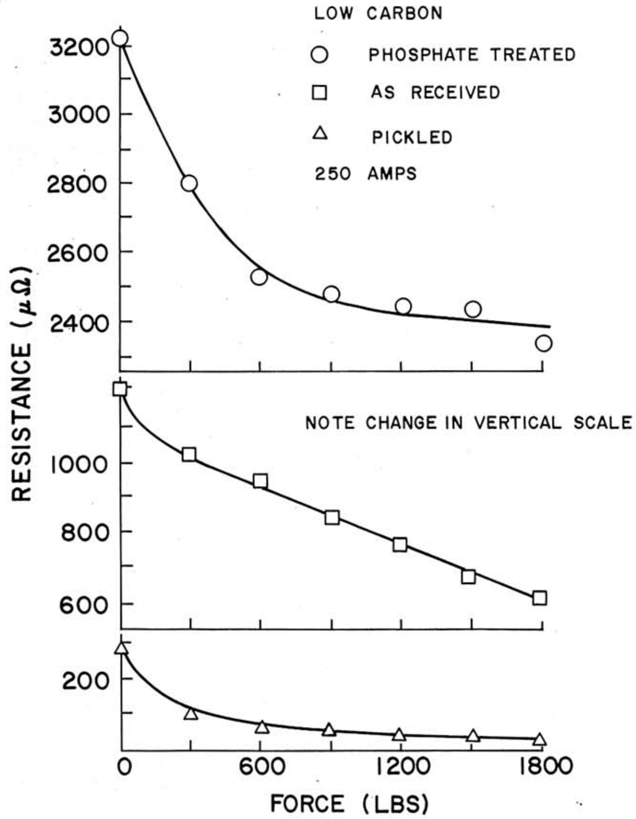

Fig. 4 — Static resistance vs. force for the low carbon steel with each surface preparation

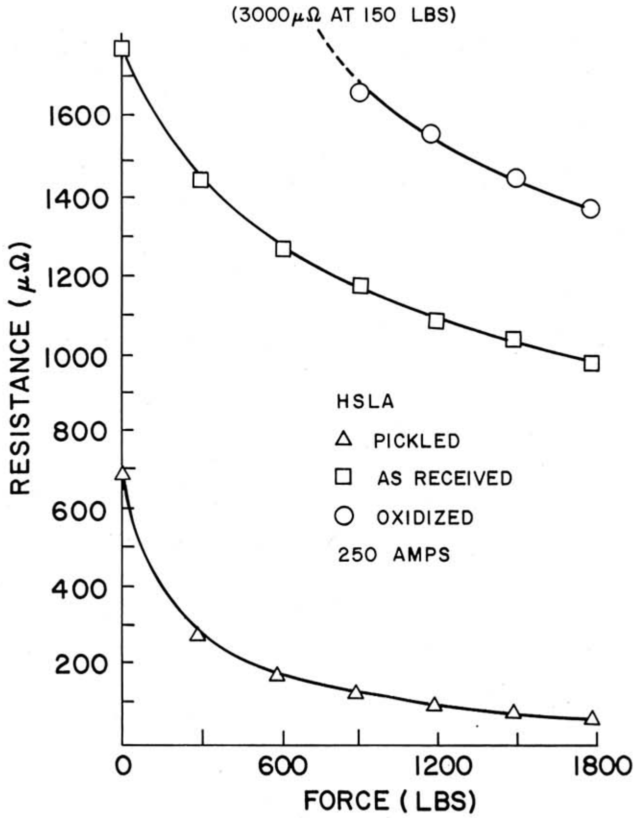

Fig. 5 — Static resistance vs. force for the HSLA steel with each surface preparation

al and current condition. Static resistance vs. current measurements were taken at a constant electrode force of 150 lb (667 N).

The same circuit was utilized in determining resistance as a function of electrode force using a DC current of 250 A. The bulk resistivity of each steel to 900°C (1652°F) was determined experimentally using a four point probe in a vacuum furnace. In one series of tests, the resistances of the electrode-sheet interfaces, R_1 and R_5, were reduced to very low levels by placing liquid gallium between the pickled outside surface of the sheet and the electrode. The total resistance values measured with R_1 and R_5 eliminated in this manner were compared with the values measured without eliminating R_1 and R_5. R_2 and R_4 were calculated from the bulk resistivity by assuming a resistive length equal to the sheet thickness and an area equal to the electrode tip. In this way the magnitude of each resistance, R_1 through R_5, could be estimated.

Dynamic Resistance Measurements

While it is important to consider the response of resistance to pressure and current, resistance spot welding is truly a dynamic process where few parameters are independent. In order to further understand the mechanisms which determine lobe shape, dynamic resistance was monitored for the matrix of welding conditions. An oscillographic recorder with 5 kHz bandwidth allowed simultaneous recording of current, electrode force and voltage. Dynamic resistance was calculated by dividing the peak voltages by the corresponding peak currents.

Results

The bulk resistivity of each steel as a function of temperature is shown in Fig. 1. It will be noted that the temperature dependence of both steels is similar but that the HSLA steel has a 40% higher room temperature resistivity. It will be shown subsequently that this difference can be substantial in terms of nugget formation.

The static resistance as a function of test current is shown in Figs. 2 and 3 for the low carbon and HSLA steels respectively. The resistance variation with force is given in Figs. 4 and 5. Estimates of the individual resistances R_1 through R_5 are

Table 2—Electrical Resistances(a) of Low Carbon and HSLA Steels

	1 R_1-R_5	2 R_2, R_3, R_4	3 $(R_1+R_5)/2$	4 R_3	5 R_2+R_4 Meas.	6 R_2+R_4 Calc.
Low carbon:						
Pickled	288 (± 31.8)(b)	122 (± 40.9)	83	51 (± 18.8)	71	10.4
As-received	1036 (± 89.0)	493 (± 66.7)	271	394 (± 41.1)	99	10.4
Phosphate	1588 (± 117)	622 (± 47.4)	483	539 (± 24.2)	83	10.4
HSLA:						
Pickled	533 (± 82.4)	321 (± 46.2)	106	170 (± 46.8)	151	14.8
As-received	1287 (± 52.0)	593 (± 32.7)	347	468 (± 25.5)	125	14.8
Oxidized	N.A.	N.A.	N.A.	N.A.	N.A.	N.A.

(a) Measured at 250 A search current.
(b) Standard deviation.

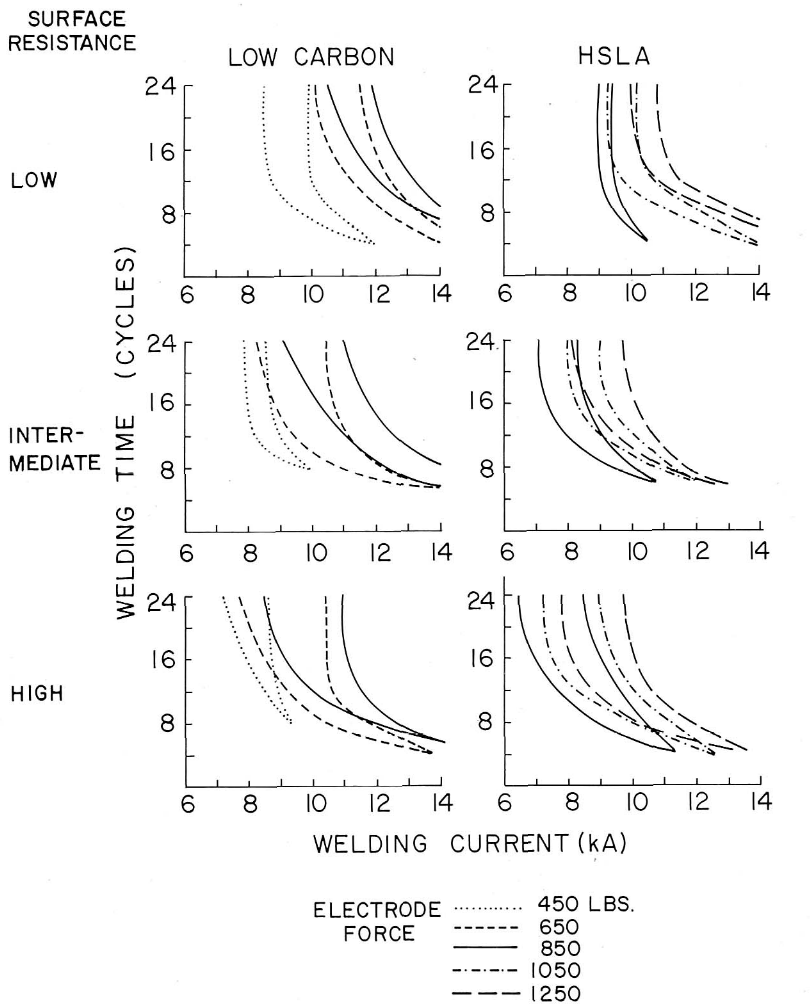

Fig. 6 — Welding lobes for both steels as a function of surface preparation and electrode force

given in Table 2. The total resistance, R_1 through R_5, is taken from Figs. 2 and 3. The sum of R_2, R_3, and R_4 was measured using liquid gallium contacts at the electrode sheet interface.

The third column of Table 2 is obtained by subtracting the second column from the first and dividing by two. R_3 is measured by attaching the voltage probes to the sheets rather than to the electrodes. This is similar to the technique used by Savage (Ref. 6). Column five is obtained by subtracting columns two and four from column one. Column six is calculated from the room temperature values of Fig. 1. The derived values in column five are relatively constant considering the large deviation in the measured values given in columns one, two and four. The large deviation between columns five and six is discussed later.

The welding lobes of both steels with each surface preparation and electrode force are shown in Fig. 6. A typical set of dynamic resistance curves superimposed on a welding lobe are shown in Fig. 7.

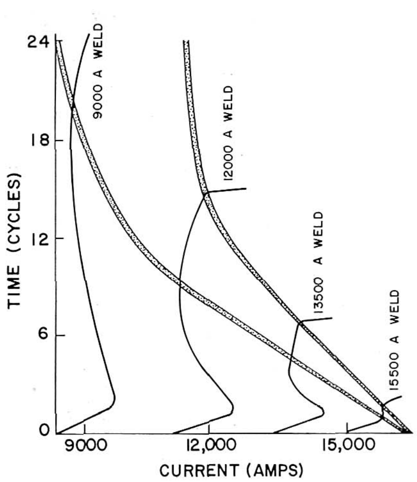

Fig. 7 — Dynamic resistance curves superimposed on a welding lobe

Discussion

Static Resistance

Static resistance measurements indicate that the contact resistance is controlled by both the surface coating and the breakdown of local contact points. It is well known that contact between two smooth surfaces, no matter how finely polished, actually occurs at a few localized points. At high magnification, the apparently smooth surface is found to be very rough. The true contact area may be as little as one to ten percent of the nominal contact area (Ref. 7). Application of pressure causes these contact points to collapse and flatten as the local yield stress is exceeded, resulting in a greater area of contact.

This is readily apparent in Figs. 4 and 5, where the contact resistance is seen to decrease with the applied force. The decrease is roughly linear beyond 600 lb (2.67 kN). The greater yield strength in the HSLA steel produces a higher surface contact resistance for an equivalent surface coating due to the smaller area under the true contact points at equal applied force.

It is felt that electrode force reduces interface resistance primarily by plastically deforming local contact points. However, with increasing surface contamination, contact resistance also becomes dependent on film breakdown. It was observed that the low pressure electrical resistance of pickled material remained constant following the application and removal of a high force, while oxidized and phosphate coated material returned to approximately 90% of the original contact resistance.

The breakdown of contact points with the application of current is apparent from the data in Figs. 2 and 3. Higher currents produce greater local heating at the contact points which in turn causes softening of metal, resulting in flattening of the contact with a reduction in the overall contact resistance. The greater resistance of the oxide and phosphate coatings results in heating and softening at lower applied currents. At very high currents all surface resistances converge toward a low value, although significant overall differences remain (note that the vertical scale of Figs. 2 and 3 is logarithmic).

Flattening of the contact points was further confirmed by the fact that the measurements were not reversible when the test current was reduced. Once a high current has been used, the resistance remained at this lower value when a lower test current was applied.

Local contacts provide an explanation for the discrepancy between columns five and six of Table 2. Using a low force and a low test current, it can be expected that the current will channel through the bulk of the material due to constriction at the local contact points. This would produce a conducting cross section in the bulk which is much smaller than the electrode contact area. At higher test currents this effect is expected to be much less.

Direct evidence of the softening and melting of local contact points is shown in Fig. 8. A large number of small, brittle fractures may be seen on the surface of a weld which was terminated before the

Fig. 8—Scanning electron micrograph of the initial formation of a weld nugget in low carbon steel made with 10,500 A, 650 lb (2.89 kN) force and 3 cycles. Note the even distribution of localized contact points. X20

nugget began to form. These fractures are most likely due to melting of the local contact points. The brittle fracture may be due to very high local oxygen caused by absorption of the surface oxides into the small liquid region; it may also be due to formation of martensite caused by the rapid cooling of these regions. Nonetheless, these features indicate that the welding current is localized at many points during the initial stages of nugget development.

Dynamic Resistance

The dynamic resistance measurements also may include reactive components as evidenced by the phase angle between the voltage and the current. Nonetheless, these dynamic resistance (reactance) measurements are related to the formation of the weld nugget. Dickinson noted a peak in the resistance which he designated by the Greek letter Β (Ref. 4). It has been observed in this study that the Β peak is more pronounced in long time welds than in short time welds. Indeed, in welds of less than five cycles the Β peak may not be apparent.

In welds in which the Β peak appears, localized melting and surface adhesion may occur several cycles prior to the Β peak. The Β peak seems to correspond to complete surface melting and to the beginning of nugget growth.

The Β peak is caused by the competing effects of increasing bulk resistivity with temperature and decreasing interface resistance. In short time welding, the increases in the temperature of the bulk may be insufficient to produce a Β peak.

Higher initial contact resistance produces a more rapid decrease in the faying interface resistance, R_3, during the weld cycle. Increased bulk resistance causes more rapid heating of the bulk. Both of these changes shift the Β peak to shorter times, which is consistent with the hypothesis that the peak is related to competition between increased bulk resistivity and decreased surface resistance.

Shifting of the Β peak to shorter times represents an increase in the rate of nugget formation. It follows that the rate of nugget development can be increased by either increasing surface resistance or by increasing welding current. Figure 7 illustrates the shift for increasing currents across a welding lobe. It is observed that increasing the welding current is directly analogous to the dynamic changes found by increasing the surface resistance.

Modeling of Heat Generation

In order to qualitatively explain the phenomena caused by variations in bulk and surface resistances, a simplified model of heat generation was constructed. This model did not consider heat loss to the electrodes. Instead, the heat generation at R_1 and R_5 was assumed to be zero. While the validity of the model is therefore limited, its qualitative value is considerable. Details of the computer program are available (Ref. 8).

The computer model treated the faying interface resistance as exponentially decreasing with temperature as suggested by Funk (Ref. 9). Bulk resistivity was varied as a function of temperature, in accordance with the data of Fig. 1.

Results obtained using the model are shown in Figure 9; they illustrate how the heating rate is affected by both surface resistance and bulk resistivity. Melting of the interface is shown to vary considerably for various surface conditions. Bulk resistivity controls bulk heating and softening and therefore, expulsion. Bulk heating in HSLA steels was found to achieve a given temperature approximately one cycle faster than in low carbon steels. The higher rate of bulk heating in HSLA steels produces earlier softening of the bulk which leads to earlier expulsion and hence narrower welding lobes.

Welding Lobe Shape

For each bulk and surface resistance tested, a low, an optimum and a high electrode force welding lobe was determined as illustrated in Fig. 6. The optimum electrode force is the one which produces the widest welding current range. It appears that the optimum force is related to the mechanical strength of the steel. Since the true area at the localized contact points is proportional to the ratio of the applied force and the

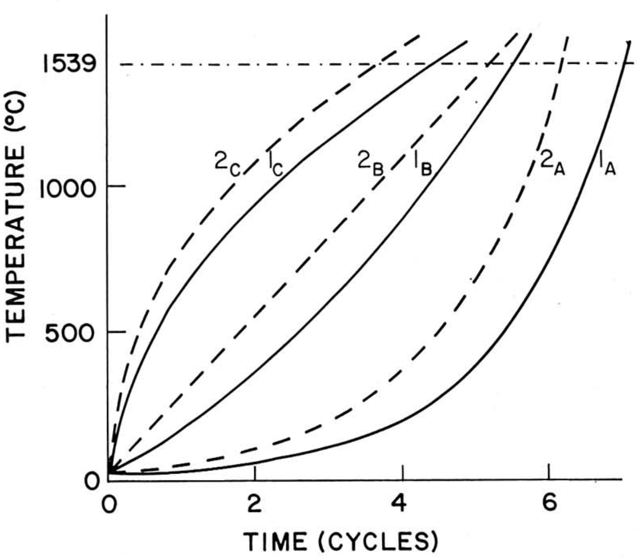

Fig. 9—Calculated heating rates at the faying surface and in the bulk for both steels with two different surface conditions. The welding current was assumed constant at 8000 A. The symbols 1A and 2A refer to the bulk heating of low carbon and HSLA steels, respectively, while 1B and 2B are the interfacial heating rates for pickled materials, and 1C and 2C are the interfacial heating rates for high surface resistance materials

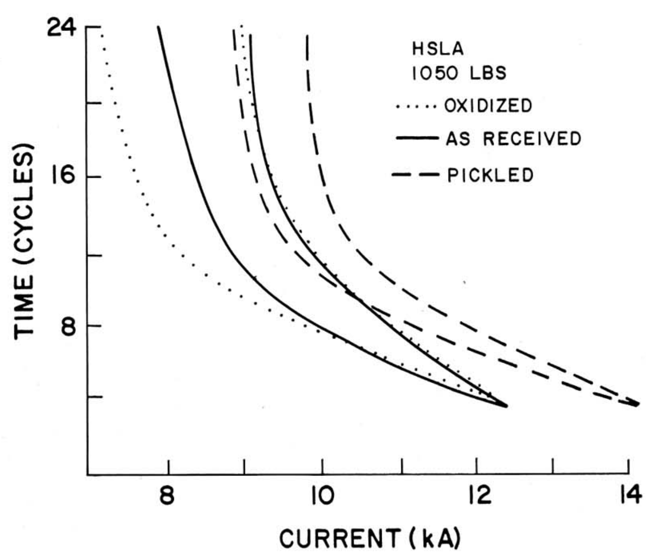

Fig. 10—Welding lobes at the optimum electrode force for HSLA steels with each surface condition

yield strength of the material, it appears that a minimum true contact area is necessary to produce the widest range of welding conditions.

Increased electrode force for all material combinations shifted the lobe to higher currents. It was also noted that increased force extended most lobes to shorter weld times.

Higher electrode forces broadened the possible range of welding currents. This is illustrated by the apparent decrease in slope of the lobes at shorter times as exemplified most clearly by the shift of the pickled HSLA lobe; nonetheless, these trends are general. Since increased electrode force can significantly reduce interface resistance, higher pressure should produce the same trends as lower surface resistance. A comparison of all welding conditions shows this to be true.

Both the minimum and the maximum lines of optimum force HSLA lobes occur at lower current values than were found for similar low carbon materials. This is expected due to the higher bulk and surface resistances of the HSLA steels. Interestingly, the HSLA lobe width was increased with higher surface resistance conditions. Higher surface resistances shifted the minimum lobe line to shorter times and lower currents. Figure 10 shows that the HSLA expulsion line remains virtually unchanged for both the as-received and oxidized conditions despite the shift of the minimum line.

The lobes of Fig. 6 and the observations made above provide sufficient information to make some general statements concerning the shape of welding lobes.

The lobe shape for any welding condition can be defined in terms of the ratio of bulk resistance to surface resistance. The position of the minimum and the maximum lobe lines is a function of these resistances, either independently or as a complex function of both. In order to examine this relationship, it is necessary to subdivide the welding lobe into several regions of interest.

Referring to Fig. 11, it is helpful to think of vertical slices of the lobe as being a series of constant current vs. time plots. In other words, for a given current, the lobe defines the necessary time, t'_2, for the interface to melt and to form an acceptable nugget. Once the initial nugget is formed, the distance between the initial nugget line and the maximum line defines the time, t_1, t_2 or t_3, that a given current can remain applied without causing excessive melting and expulsion. It should be remembered that $R_3 = 0$ at the initial nugget line; hence, bulk heating effects predominate inside the lobe.

It is useful to qualitatively examine the temperature profile across the steel sheets during welding. Initially, the high faying surface resistance creates a steep temperature gradient between the interface and the bulk material. With increasing time, bulk material is heated by its own resistance as well as by thermal conduction due to heat generated at the faying interface.

Heat generated at the electrode-sheet interface may be substantial; however, this does not significantly influence bulk temperature due to the ability of the adjacent electrode to serve as a heat sink. Referring to Fig. 12, one can see how the ratio of interface and bulk resistances can affect the shape of the temperature profile.

The time necessary for the faying interface to reach the melting point is related to the magnitude of the interface resistance. Once the faying surface has melted, the interface resistance is reduced to zero and R_3 no longer affects weld development. Expulsion, on the other hand, is caused by the thermal softening of solid metal adjacent to the weld nugget. The temperature of this sealing material (T_{seal} in Fig. 12) is critical in expulsion determination. In this way expulsion is directly a function of bulk resistivity as suggested by Yamanchi and Taka (Ref. 2)). This relationship is more pronounced at longer welding times.

For very short welding times, it is proposed that high currents cause very rapid heating of the faying interface and in effect, superheat adjacent material before a seal can be formed. This occurs at very short times where the diffusion of heat from the interface to the bulk is limited. Hence, two scenarios for expulsion may be considered:

1. For longer time welds, expulsion

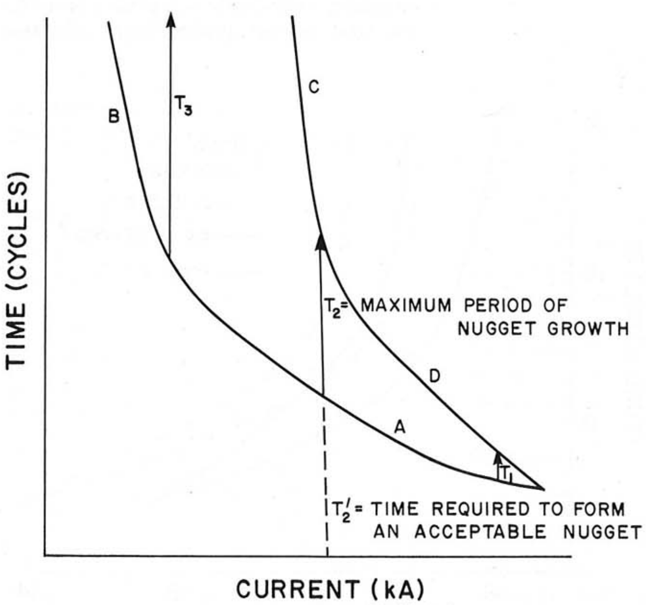

Fig. 11 — Schematic welding lobe illustrating the four regions of nugget formation and expulsion described in the text. The times t_1, t_2, and t_3 are nugget growth parameters. t'_2 is the time for the nugget to begin to form

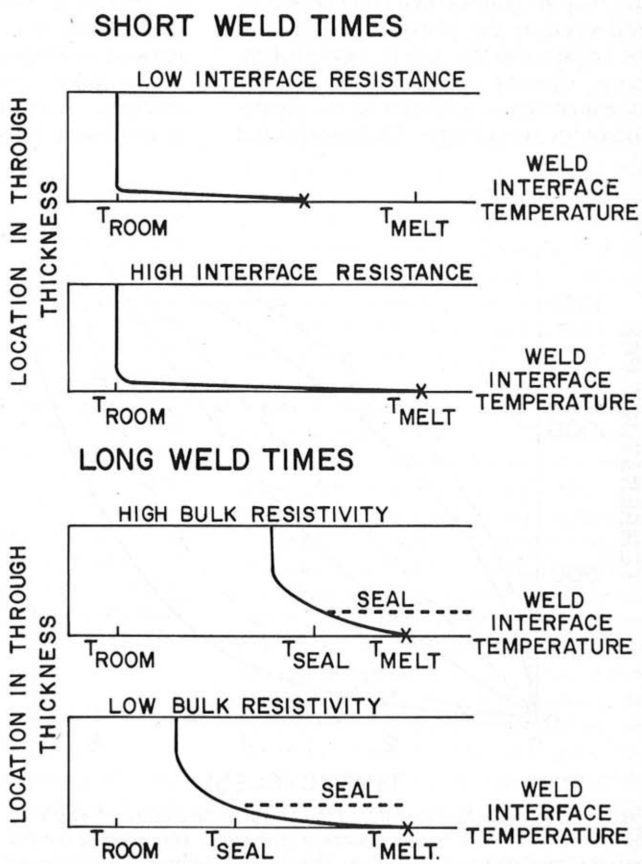

Fig. 12 (right) — Schematic temperature profiles through the sheet thickness at short and long weld times in material of both high and low interface resistance will be caused by softening of the seal material due to bulk resistive heating.

2. *Short time welding can result in* what could be called "flash expulsion," where excessive interfacial heating occurs at a rate much greater than the rate of heat dissipation. Flash expulsion can also occur in low current welds where interface resistance is extremely high. Here again, expulsion is caused by excessive interfacial heating, without softening the sealing material surrounding the nugget.

Referring again to Fig. 11, each section of the lobe is controlled by various resistance parameters. These relationships are discussed separately below.

Region A of Fig. 11 is determined primarily by heat generation at the faying interface, i.e., $I^2 \cdot R_3$. The greater the value of R_3 the earlier a nugget will begin to form. The lobes of Fig. 6 confirm that lower surface resistances or higher electrode forces shift region A to higher welding currents and shorter weld times (i.e., narrowing the distance between region A and region D of Fig. 11).

Region B of Fig. 11 is controlled by the ratio of surface resistance to bulk resistance. At very low surface resistance values, the rate of heat generation is low and heat loss through the bulk at these longer weld times can equal the rate of surface heat generation. The line in region B will become nearly vertical, and it becomes impossible to form a nugget below a minimum welding current. As the surface resistance is increased, the rate of heat generation exceeds the rate of heat loss and sufficient time will allow a nugget to form. Hence, higher surface resistances cause region B to shift to lower welding times. Again, the lobes in Fig. 6 are consistent with this pattern.

Expulsion at moderate to long weld times in region C of Fig. 11 is caused by softening of the restraining material adjacent to the molten nugget. As noted previously, this softening is controlled by the bulk resistivity of the steel. HSLA steels, with higher bulk resistivities, produce expulsion at lower currents or alternatively, closer to the A and B regions. This produces a narrower welding lobe width.

The lower expulsion region D of Fig. 11, is produced by a different mechanism than in region C. In C, the bulk overheats and softens, allowing molten metal to escape. In region D, which is separated from C by a transition region, the rapid surface heating caused by the high welding current produces melting before the bulk has heated sufficiently to form an outer seal which can retain the molten metal. More is said about this in the following section.

Mechanics of Nugget Development

In order to further understand the instabilities created in short time welding, the mechanics of nugget growth were studied for high, medium and low welding currents. Scanning electron microscopy revealed that a separate mode of nugget development is associated with each.

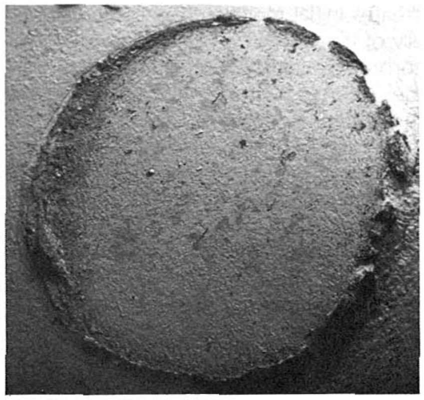

Fig. 13 — Peripheral melting of a low carbon steel weld made at 24,500 A, 650 lb (2.89 kN) force and 1 cycle welding time. X20

At very high currents and short welding times (region D of Fig. 11), the initial melting of the faying surface occurs around the periphery of the electrode — Fig. 13. At these very short times, expulsion occurs either before an acceptable nugget is formed or immediately after. Acceptable nuggets were formed by this mode only for the lower surface resistance conditions of HSLA pickled, and low carbon pickled and as-received material. Significant expulsion was always present, although nuggets could be created in HSLA as-received, oxidized and low carbon phosphate treated material. Hence, the slower heating rates of lower surface resistance materials are apparently more conducive to stable peripheral melting. The lower rate of surface heating allows time for the bulk material to reach the seal temperature.

It is believed that peripheral melting is due to the fact that the outermost surface of the contact area is under the least triaxial constraint. Therefore, this surface will be most easily deformed and will offer a low resistance current path. The use of domed electrodes may counteract this phenomena and allow for more successful welding at higher currents and shorter times. This can be substantiated by the use of such electrodes in the welding of aluminum where a high ratio of surface resistance to bulk resistance is present.

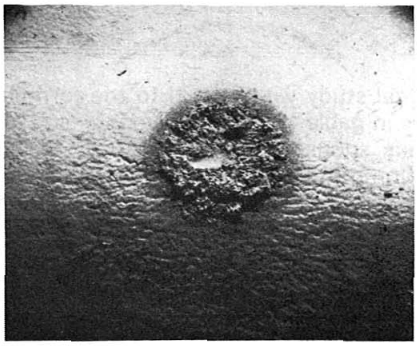

Fig. 14 — Radial nugget growth in low carbon steel weld made at 7,250 A, 650 lb (2.89 kN) force and 24 cycle welding time. X20

At lower surface currents, breakdown and current flow become more uniform across the interface. This is shown in Figs. 8 and 14. For these lower current welds, peripheral melting is absent. Figure 8 illustrates early nugget development for a weld below the minimum nugget diameter line at t'_2 of Figure 11. The independent points of contact scattered evenly across the interface have been noted previously. Each individual cleavage fracture represents welding between the two sheets. Continued application of welding current would result in the coalescence of these individual welds.

Figure 14 shows the underdeveloped nugget of a low current, long time weld. The entire contact surface has melted on each sheet, however, the actual weld nugget is seen growing radially from the central region. This geometry is believed to be created by the radial temperature gradients which occur at long welding times due to diffusion of heat throughout the bulk. In these situations, heat is flowing radially outward into the sheets, and the center of the weld is the hottest and, therefore, the first region to melt.

Summary

The results of the study presented above suggest that there exists an optimum ratio of surface to bulk resistance, which will produce material with the widest range of welding current. Although little can usually be done to alter the resistivity of the base metal, cleaning or coating the sheet to alter the surface resistance can produce significant changes in the welding performance. In the case of the HSLA steel, a higher resistance coating has increased the welding current range to acceptable levels, while it has hardly affected the low carbon steel. A material such as aluminum with a very low bulk resistivity requires a very low surface resistance in order to provide the proper balance between surface and bulk heating. Most expulsion in aluminum spot welding is thought to be of the same form as that observed in Region D of Figure 11.

A further advantage of increasing the surface resistance of HSLA steel is a 20% reduction in electrode force which is permissible without a reduction in the width of the welding lobe. This decrease in force reduces the tendency for tip mushrooming during long production use. Another benefit is a marked reduction in the incidence of interfacial failure of the weld nuggets. Although the cause of this is not known, it may be related to the increased heating and decreased cooling rates produced by the high resistance interfaces.

Conclusions

The experimental results of this study have disclosed some of the fundamental principles determining lobe shape determination. The following conclusions have been drawn concerning the resistance spot welding of HSLA and low carbon steels:

1. HSLA steels exhibit both higher bulk resistivities and surface resistances than similarly treated low carbon steels.
2. Electrode-sheet interface resistances are comparable in value to faying interface resistances; however, the heat generated at the former interfaces is primarily dissipated into the electrodes.
3. The actual area of current flow may vary markedly from the nominal area of contact. The lower the current or the shorter the weld time, the more this discrepancy will be accentuated.
4. The B peak of the dynamic resistance curve is shifted to earlier times in the weld sequence by increasing either the weld current or the surface resistance.
5. The significance of the B peak is diminished as weld time is decreased.
6. High current, short time welding creates initial melting around the periphery of the contact area. Moderate to low current welding creates more uniform melting across the contact area, causing the nugget to grow radially outward.
7. Higher electrode forces require welding at higher currents but allow for stable welding at shorter times.
8. The trends of lobe shape modification observed for lower surface resistance materials are analagous to the trends observed for higher electrode force welding.
9. HSLA lobe width can be increased by treating the surface with a high resistance oxide coating. Such a treatment also improves nugget failure characteristics and permits the use of lower electrode forces.

The experimental results of this study have only confirmed these conclusions for the welding of low carbon and HSLA steels. Nonetheless, it is believed that the heat generation balance as determined by the relative magnitude of surface resistance and bulk resistivity is generally applicable to all metals.

Acknowledgments

The authors are very grateful to Bethlehem Steel Corporation for financial support of this work. In particular, Drs. J. C. Baker and J. M. Sawhill, Jr., have provided encouragement and support. The phosphate coating was provided by Amchem Corporation of Ambler, Pennsylvania.

References

1. Sawhill, J. M., Jr., and Baker, J. C. 1980. Spot weldability of high-strength sheet steels. *Welding Journal* 59(1): 19-s to 30-s.
2. Yamanchi, N., and Taka, T. *Spot weldability of high tensile strength sheet steel.* IIW doc. III-644-80.
3. Sawhill, J. M., Jr.; Watanabe, H.; and Mitchell, J. W. 1977. Spot weldability of Mn-Mo-Cb, V-N and SAE 1008 steels. *Welding Journal* 56(7): 217-s to 224-s.
4. Dickinson, D. W.; Franklin, J. E.; and Stanya, A. 1980. Characterization of spot welding behavior by dynamic electrical resistance monitoring. *Welding Journal* 59(6): 170-s to 176-s.
5. Savage, W. F.; Nippes, E. F.; and Wassell, F. A. 1978. Dynamic contact resistance of series spot welds. *Welding Journal* 57(2): 43-s to 50-s.
6. Savage, W. F.; Nippes, E. F.; and Wassell, F. A. 1977. Static contact resistance of series spot welds. *Welding Journal* 56(11): 365-s to 370-s.
7. Rabinowicz, E. 1965. *Friction and wear of materials.* New York: John Wiley.
8. Kaiser, J. G. 1980 (September). M.S. thesis. Cambridge, Massachusetts: Massachusetts Institute of Technology.
9. Rice, W., and Funk, E. J. 1967. An analytical investigation of the temperature distributions during resistance welding. *Welding Journal* 46(4): 175-s to 186-s.